Flux-Based Ozone Risk Assessment for a Plant Injury Index (PII) in Three European Cool-Temperate Deciduous Tree Species

Yasutomo Hoshika [1],*, Elisa Carrari [1], Barbara Mariotti [1], Sofia Martini [1], Alessandra De Marco [2], Pierre Sicard [3] and Elena Paoletti [1]

[1] Institute of Research on Terrestrial Ecosystems (IRET), National Research Council of Italy (CNR), Via Madonna del Piano, I-50019 Sesto Fiorentino, Italy; eli.carrari@gmail.com (E.C.); barbara.mariotti@unifi.it (B.M.); sof.martini@outlook.com (S.M.); elena.paoletti@cnr.it (E.P.)

[2] Italian National Agency for New Technologies, Energy and the Environment, C.R. Casaccia, 00123 Rome, Italy; alessandra.demarco@enea.it

[3] ARGANS, 260 Route du Pin Montard, BP 234, 06904 Sophia Antipolis, France; psicard@argans.eu

* Correspondence: yasutomo.hoshika@cnr.it; Tel.: +39-055-522-5949; Fax: +39-055-522-5920

check for updates

Abstract: This study investigated visible foliar ozone (O_3) injury in three deciduous tree species with different growth patterns (indeterminate, *Alnus glutinosa* (L.) Gaertn.; intermediate, *Sorbus aucuparia* L.; and determinate, *Vaccinium myrtillus* L.) from May to August 2018. Ozone effects on the timing of injury onset and a plant injury index (PII) were investigated using two O_3 indices, i.e., AOT40 (accumulative O_3 exposure over 40 ppb during daylight hours) and POD_Y (phytotoxic O_3 dose above a flux threshold of Y nmol m^{-2} s^{-1}). A new parameterization for POD_Y estimation was developed for each species. Measurements were carried out in an O_3 free-air controlled exposure (FACE) experiment with three levels of O_3 treatment (ambient, AA; 1.5 × AA; and 2.0 × AA). Injury onset was found in May at 2.0 × AA in all three species and the timing of the onset was determined by the amount of stomatal O_3 uptake. It required 4.0 mmol m^{-2} POD_0 and 5.5 to 9.0 ppm·h AOT40. As a result, *A. glutinosa* with high stomatal conductance (g_s) showed the earliest emergence of O_3 visible injury among the three species. After the onset, O_3 visible injury expanded to the plant level as confirmed by increased PII values. In *A. glutinosa* with indeterminate growth pattern, a new leaf formation alleviated the expansion of O_3 visible injury at the plant level. *V. myrtillus* showed a dramatic increase of PII from June to July due to higher sensitivity to O_3 in its flowering and fruiting stage. Ozone impacts on PII were better explained by the flux-based index, POD_Y, as compared with the exposure-based index, AOT40. The critical levels (CLs) corresponding to PII = 5 were 8.1 mmol m^{-2} POD_7 in *A. glutinosa*, 22 mmol m^{-2} POD_0 in *S. aucuparia*, and 5.8 mmol m^{-2} POD_1 in *V. myrtillus*. The results highlight that the CLs for PII are species-specific. Establishing species-specific O_3 flux-effect relationships should be key for a quantitative O_3 risk assessment.

Keywords: visible foliar ozone injury; European alder; mountain ash; European blueberry; stomatal ozone flux; free-air ozone exposure

1. Introduction

Tropospheric ozone (O_3) is one of the major concerns for forest health due to its phytotoxicity [1]. Despite the fact that peak O_3 concentrations have tended to decrease in the eastern part of United States and some European countries due to precursor emission controls [2], the global background O_3 concentration still remains high enough to cause negative impacts on tree physiology [3].

Visible foliar injury by O_3 (O_3 visible injury) is the first unequivocal visually detectable sign of O_3 damage and indicates an impairment of leaf physiological functions [4]. Hoshika et al., 2012a [5] reported that the percent of surface injury was negatively correlated with leaf gas exchange rate, highlighting a reduced photosynthesis and loss of stomatal control in poplar leaves with more than 5% injury. Ozone visible injury has been broadly investigated in native and exotic trees, shrubs, and herbs in Asia, Europe, and North America, and partly validated under controlled conditions [6–8].

An exposure-based index such as AOT40 (accumulated exposure over a threshold of 40 ppb) is used to assess O_3 risks to European forest trees [9,10]. Previous studies have reported an AOT40-based assessment of the first symptom onset of O_3 visible injury in field [11,12] or open-top chambers [13,14]. Those studies suggested that an O_3 critical level (CL) by 5 to 10 ppm·h AOT40 could protect the sensitive tree species from O_3 visible injury. However, it has been recognized that O_3 damage depends on stomatal O_3 uptake rather than only O_3 exposure [15]. To improve our quantitative assessment of O_3 effects on trees, a stomatal O_3 flux-based index such as POD_Y (phytotoxic ozone dose above a flux threshold of Y nmol m^{-2} s^{-1}) has been the focus. POD_Y is estimated using the deposition of ozone and stomatal exchange model (DO3SE) [16]. Sicard et al., 2016 [17] estimated POD_Y using the DO3SE model and analyzed field observation data in Southeastern France and Northwestern Italy. They proposed the stomatalflux-based standard to assess O_3 visible injury for two deciduous species (*Fagus sylvatica* and *Fraxinus excelsior*) and two conifer species (*Pinus cembra* and *P. halepensis*) as representative O_3 sensitive species (approximately 20 mmol m^{-2} of POD_0 corresponded to 5% injury). Many symptomatic species have been recorded in field monitoring campaigns [8,18,19]. Paoletti et al., 2019 [8] recently found O_3 visible injury in 23 tree species across forest sites in France, Italy, and Romania. Nevertheless, knowledge is still limited on species-specific model parameters to calculate stomatal O_3 uptake for establishing the O_3 flux-effect relationship in most symptomatic tree species.

The species-specific tree response to O_3 can be affected by the growth pattern (i.e., indeterminate or determinate) [20]. In elevated O_3, the tree species with indeterminate pattern (e.g., poplar) can initiate new leaf formation to replace damaged older leaves [21]. This response can limit the development of O_3 visible injury at the plant level for those species. In this study, we selected three European cool-temperate deciduous tree species with different growth patterns, i.e., *Alnus glutinosa* (L.) Gaertn. (indeterminate) [22], *Sorbus aucuparia* L. (intermediate) [23], and *Vaccinium myrtillus* L. (determinate) [24]. These three species have often shown O_3 visible injury in field forest sites [8]. The aim of this study was to achieve the species-specific parameterization of the DO3SE model in these three tree species, examining both the onset date of O_3 visible injury and its expansion at the whole plant level using a plant injury index (PII) [4] in an O_3 free-air controlled exposure (O_3 FACE) experiment. The PII can be more closely related to the plant physiological status and especially whole plant carbon loss than to first symptom onset [14]. Three hypotheses were tested as follows: (i) Are species with higher stomatal O_3 uptake more sensitive to O_3? (ii) Does the tree growth pattern affect the expansion of O_3 visible injury at plant level? and (iii) Is the flux-based approach better than the exposure-based one to explain the PII?

2. Materials and Methods

2.1. Experimental Site and Plant Material

Measurements were conducted at an O_3 FACE facility located in Sesto Fiorentino, in central Italy (43° 48′ 59″ N, 11° 12′ 01″ E, 55 m a.s.l.). The details of the system are described in Paoletti et al., 2017 [25]. Five-year old saplings of *A. glutinosa* and *S. aucuparia*, and three-year old saplings of *V. myrtillus* were obtained from a nearby nursery in December 2017. Plants were transplanted into plastic pots (50 L for *A. glutinosa* and *S. aucuparia* and 25 L for *V. myrtillus*) containing a mixture of sand:peat:soil = 1:1:1 (*v:v:v*). In 2018, plants were exposed to the following three levels of O_3 concentration: Ambient air (AA), 1.5 times ambient O_3 concentration (1.5 × AA), and twice ambient O_3 concentration (2.0 × AA). Three replicated blocks (5 m × 5 m × 2 m) were set to each O_3 treatment

(n = 3) with three (*A. glutinosa* and *S. aucuparia*) or six (*V. myrtillus*) plants (total 27 plants for *A. glutinosa* and *S. aucuparia*, and 54 plants for *V. myrtillus*). Ozone concentrations in each treatment were recorded continuously by an O_3 monitor (Mod. 202, 2B Technologies, Boulder, CO, USA). All plants were irrigated to keep field capacity at 1- to 3-day intervals to prevent water stress. We monitored the light intensity, relative humidity, air temperature, precipitation, and wind speed above the O_3 FACE facility (2.5 m height) using a WatchDog meteorological station (Model 2000, Spectrum Technologies, Inc., Aurora, IL, USA).

2.2. Assessment of Ozone Visible Injury

The onset of O_3 visible injury was assessed every 2 to 3 days in May 2018. After we found the first symptom in any O_3 treatment, the percentage of symptomatic leaves per plant (LA) and the percentage injured area in the symptomatic leaves (AA) were scored (*A. glutinosa* on 31 May, 21 June, 10 and 21 July, and 8 and 20 August; *S. aucuparia* on 31 May, 21 June, 10 July, and 8 and 20 August; *V. myrtillus* on 31 May, 21 June, 4, and 11 and 19 July) with a ×10 hand lens and the help of photoguides (Innes et al. 2001 and Paoletti et al. 2009). All attached leaves were scored and counted by the same two observers. To assess the whole plant injury, a PII was calculated combining the two parameters, PII $=$ (LA × AA)/100 [4].

2.3. Modeling of Stomatal Conductance

Leaf gas exchange was measured in fully expanded sun-exposed leaves (1 to 3 plants per replicated plot per each O_3 treatment) using a portable infrared gas analyzer (CIRAS-2 PP Systems, Herts, UK). Measurements were made on the days with clear sky in the morning (8 h to 10 h), afternoon (13 h to 15 h) and evening (16 h to 19 h) from May to October 2018. Natural illumination was used for the measurement. The CO_2 concentration in the chamber (Ca) was set to 400 ppm. The temperature and relative humidity in the chamber were adjusted manually to the ambient condition. Pooled data (210 for *A. glutinosa*, 217 for *S. aucuparia*, and 216 for *V. myrtillus*) were used to estimate the parameters of the DO3SE model [16], as follows:

$$g_s = g_{max} \times f_{phen} \times f_{light} \times \left\{ f_{min,} \quad \left(f_{temp} \times f_{VPD} \times f_{SWC} \right) \right\} \tag{1}$$

where g_{max} is the maximum stomatal conductance, i.e., mmol O_3 m^{-2} projected leaf area (PLA) s^{-1}. The other functions are all expressed as relative terms and are scaled from 0 to 1. The model accounts for the minimum stomatal conductance (f_{min}) and the variation in g_s according to phenology (f_{phen}), photosynthetic photon flux density (PPFD) (f_{light}), temperature (f_{temp}), vapor pressure deficit (VPD) (f_{VPD}), and soil water content (f_{SWC}). The f_{SWC} was not applied in this study (f_{SWC} = 1) because the soil moisture was equivalent to field capacity. The g_{max} and f_{min} values were set as 95th and 5th percentile values recorded in the experiment. Parameterizations of other functions were carried out using a boundary line analysis [26,27]. Further details on $f_{phen}, f_{light}, f_{temp,}$ and f_{VPD} calculations are provided in CLRTAP (2017) [16].

2.4. Calculation of Ozone Indices

AOT40 was calculated by using hourly O_3 concentrations during daylight hours (short wave radiation > 50 W m^{-2}) according to CLRTAP (2017) [16]. It is given by:

$$AOT40 = \sum_{i=1}^{n} max\left([O_3]_i - 40, \quad 0 \right) \tag{2}$$

where $[O_3]_i$ is the ith measured hourly O_3 concentration (ppb) with i equal to 1 … n in the integral and n is the number of hours included in the calculation period.

Stomatal O_3 uptake (F_{st}, nmol m^{-2} s^{-1}) was calculated as:

$$F_{st} = [O_3] \times g_s \times \frac{r_c}{r_b + r_c} \tag{3}$$

where r_c is the leaf surface resistance (= $1/(g_s + g_{ext})$, s m^{-1}), g_{ext} is the external leaf or cuticular conductance (s m^{-1}) [16], and r_b is the leaf boundary layer resistance, given as:

$$r_b = 1.3 \times 150 \times (L_d/u)^{0.5} \tag{4}$$

where u is wind speed (m s^{-1}) and L_d is the species-specific leaf dimension (*A. glutinosa* 0.07 m, *S. aucuparia* 0.04 m, and *V. myrtillus* 0.04 m obtained as averaged value of 3 to 5 leaves of two plants in each block in each O_3 treatment) [16].

POD_Y (mmol m^{-2}) was estimated from hourly data as:

$$POD_Y = \sum_{i=1}^{n} \max\left(F_{st\_i} - Y, \ 0 \right) \tag{5}$$

where F_{st_i} is the ith hourly stomatal O_3 uptake (nmol m^{-2} s^{-1}) and n is the number of hours included in the calculation period. Y is a species-specific threshold of stomatal O_3 uptake (nmol m^{-2} s^{-1}).

Exposure- or flux-based dose-response functions were determined from a linear regression between PII and AOT40 or POD_Y over a threshold of Y (Y from 0 to 10, with an increment of 0.5 nmol m^{-2} s^{-1}). Two criteria were applied to select the best dose-response function which included: (1) the confidence interval (C.I.) must include Y-intercept = 0, and (2) among the functions meeting criterion 1, the equation with the highest R^2 value was chosen. CLs were calculated as the level when PII reaches 5. In fact, a significant decline of physiological performance was found in leaves with more than 5 of PII [14].

2.5. Data Analysis

Statistical analyses were performed using SPSS (20.0, SPSS, Chicago, IL, USA). To assess the effects of O_3 on the number of attached leaves, a two-way analysis of variance (ANOVA) was applied. Data were checked for normal distribution and homogeneity of variance (Levene's test). Since the PII data were not normally distributed, the Kruskal–Wallis analysis of variance was applied to examine the effect of O_3. The relationships between PII and O_3 indices were fitted using a simple linear regression. Results were considered significant at $p < 0.05$.

3. Results

3.1. Ozone Concentration and Meteorological Factors

Daily mean PPFD, air temperature, wind speed, and relative humidity (mean ± S.E.) during the exposure period (May to October 2018) were 527 ± 13 µmol m^{-2} s^{-1}, 22.8 ± 0.3 °C, 0.3 ± 0.0 m s^{-1}, and 55.6% ± 0.8%, respectively (Figure 1). Total rainfall was 136 mm. Daily mean O_3 concentration (mean ± S.E.) in AA, 1.5 × AA, and 2.0 × AA was 35.2 ± 0.7 ppb, 53.1 ± 1.1 ppb, and 65.2 ± 1.4 ppb, respectively.
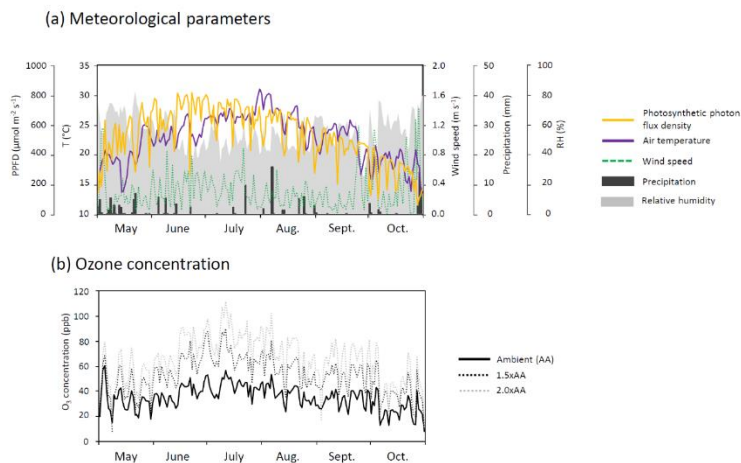
Figure 1. Meteorological factors and O_3 concentration over the experimental period (from May to October 2018) showing daily mean values of photosynthetic photon flux density (PPFD), air temperature (T), wind speed, precipitation, relative humidity (RH), and the following three levels of ozone concentrations at the O_3 FACE: Ambient air (AA), 1.5 times ambient O_3 concentration ($1.5 \times$ AA), and twice ambient O_3 concentration ($2.0 \times$ AA).

3.2. Ozone Visible Injury

The first O_3 visible injuries were observed in $2.0 \times$ AA on 18 May for *A. glutinosa*, on 21 May for *S. aucuparia*, and on 26 May for *V. myrtillus* (Table 1). Ozone visible injury occurred as dark or reddish stippling on the upper leaf surface (Figure 2) and was more severe in older than in younger leaves. The AOT40 corresponding to the onset of O_3 visible injury was 5.6 to 8.9 ppm·h, and the POD_0 corresponding to the occurrence of injury was approximately 4.0 mmol m^{-2} regardless of tree species. After the onset of O_3 visible injury, the PII value increased in all species (Figure 3) due to an increased number of symptomatic leaves and injured leaf area (data not shown). Ozone significantly increased PII values in *A. glutinosa* on 21 June ($1.5 \times$ AA, +224% and $2.0 \times$ AA, +656%), 8 August ($1.5 \times$ AA, +400% and $2.0 \times$ AA, +1163%), and 20 August ($1.5 \times$ AA, +440% and $2.0 \times$ AA, +2169%). Ozone-induced increases of PII were also found in *S. aucuparia* on 20 August ($1.5 \times$ AA, +101% and $2.0 \times$ AA, +182%) and *V. myrtillus* on 19 July ($1.5 \times$ AA, +65% and $2.0 \times$ AA, +172%). Ozone stimulated the number of attached leaves in *A. glutinosa* on 20 August (Figure 4); however, such an increase was not found in *S. aucuparia* and *V. myrtillus*.

Table 1. The date of first symptom onset of O_3 visible foliar injury and corresponding ozone indices (POD_0, phytotoxic ozone dose above a flux threshold of 0 nmol m^{-2} s^{-1} and AOT40, accumulated exposure over a threshold of 40 ppb) for *Alnus glutinosa*, *Sorbus aucuparia,* and *Vaccinium myrtillus* in $2.0 \times$ AA (twice ambient O_3 concentration).

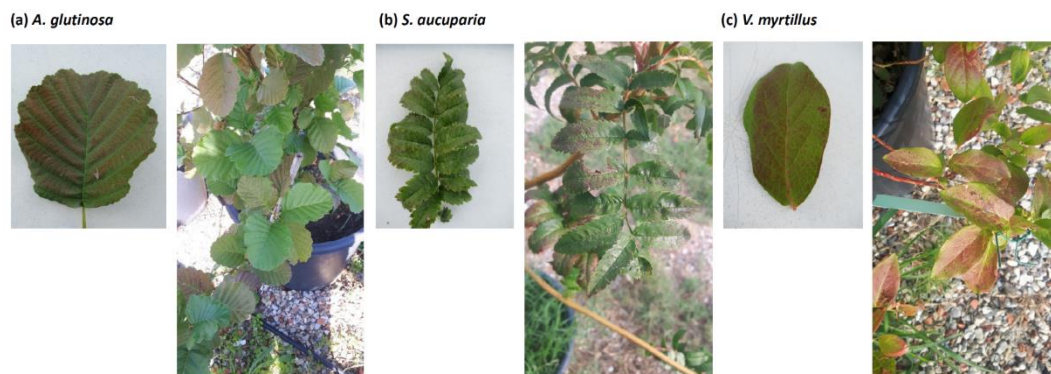| Species	*A. glutinosa*	*S. aucuparia*	*V. myrtillus*
Onset date	18 May	21 May	26 May
POD_0 (mmol m^{-2})	3.2	4.3	3.5
AOT40 (ppm·h)	5.6	6.3	8.9

Figure 2. Photographs of symptomatic leaves in *Alnus glutinosa*, *Sorbus aucuparia,* and *Vaccinium myrtillus* in an O_3 FACE experiment in 2018. Dark or reddish stippling on the upper leaf surface was found.
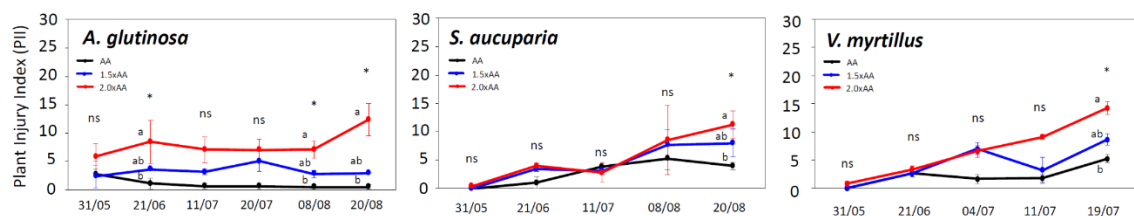

Figure 3. Plant injury index (PII) in *Alnus glutinosa*, *Sorbus aucuparia,* and *Vaccinium myrtillus* exposed to three levels of O_3 concentration (AA, ambient O_3 concentration $1.5 \times$ AA, and ambient O_3 concentration $2.0 \times$ AA). The points represent mean ± S.E. (*n* = 3 plots). Asterisks show the significance of Kruskal–Wallis tests: * *p* < 0.05 and ns, not significant. Different letters show significant differences among treatments in each date (*p* < 0.05, Mann–Whitney U test).
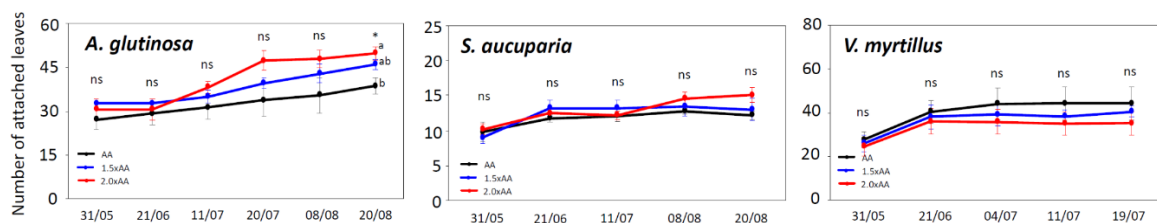

Figure 4. Number of attached leaves in *Alnus glutinosa*, *Sorbus aucuparia,* and *Vaccinium myrtillus* exposed to three levels of O_3 concentration (AA, ambient O_3 concentration $1.5 \times$ AA, and ambient O_3 concentration $2.0 \times$ AA). The points represent mean ± S.E. (*n* = 3 plots). Asterisks show the significance of ANOVA tests: * *p* < 0.05 and ns, not significant. Different letters show significant differences among treatments in each date (*p* < 0.05, Tukey test).

3.3. Parameterization of Stomatal Conductance Model

The g_{max} value was 300, 240, and 140 mmol m^{-2} s^{-1} in *A. glutinosa*, *S. aucuparia*, and *V. myrtillus*, respectively (Table 2 and Figure 5). The f_{min} values were similar in all three species, i.e., 0.13 to 0.17. The response of g_s to PPFD (f_{light}) indicated that *V. myrtillus* had a higher *a* value (0.0104) relative to *A. glutinosa* (0.0024) and *S. aucuparia* (0.0043). The optimal temperature for stomatal opening was 20 to 30 °C in all species. A VPD higher than around 1 kPa induced stomatal closure regardless of the species. The f_{phen} values peaked from June to August in all three species. Estimated g_s values were in good agreement with the measured values as confirmed by the coefficient of determination (R^2 = 0.46 to 0.61) and root mean square error (RMSE = 31 to 57 mmol O_3 m^{-2} s^{-1}) (Figure S1).

Table 2. Summary of parameters in the DO3SE stomatal conductance model for *Alnus glutinosa*, *Sorbus aucuparia,* and *Vaccinium myrtillus*.

Parameter		Unit	*A. glutinosa*	*S. aucuparia*	*V. myrtillus*
g_{max}		(mmol O_3 m^{-2} PLA s^{-1})	300	240	140
f_{min}		(fraction)	0.13	0.17	0.17
	A_{start}	(day of year)	121	121	121
	A_{end}	(day of year)	304	304	304
f_{phen}	f_{phen_a}	(days)	50	50	50
	f_{phen_b}	(days)	50	50	50
	f_{phen_c}	(fraction)	0.3	0.3	0.3
	f_{phen_d}	(fraction)	0.3	0.3	0.3
f_{light}	a	(constant)	0.0024	0.0043	0.0104
f_{temp}	T_{opt}	(°C)	29	23	20
	T_{min}	(°C)	5	0	5
	T_{max}	(°C)	40	40	40
f_{VPD}	VPD_{max}	(kPa)	1.8	1.2	1.2
	VPD_{min}	(kPa)	5.7	7.0	4.7

g_{max} is the maximum stomatal conductance; f_{min} is a fraction of minimum stomatal conductance to g_{max}; f_{phen} is the variation of stomatal conductance with season; f_{light}, f_{temp}, and f_{VPD} depend on photosynthetically relevant photon flux density at the leaf surface (PPFD, µmol m^{-2} s^{-1}), temperature (T, °C), and vapor pressure deficit (VPD, kPa), respectively; A_{start} and A_{end} are the year days for the start and end of the experiment; f_{phen_a} and f_{phen_b} represent the number of days of f_{phen} to reach its maximum and the number of days during the decline of f_{phen} to the minimum value, respectively; f_{phen_c} and f_{phen_d} represent maximum fraction of f_{phen} at A_{start} and A_{end}, respectively; a is the parameter determining an exponential curve of stomatal response to light; T_{opt}, T_{min}, and T_{max} denote optimal, minimum, and maximum temperature for stomatal opening, respectively; and VPD_{min} and VPD_{max} denote the threshold of VPD for attaining minimum and full stomatal opening, respectively.
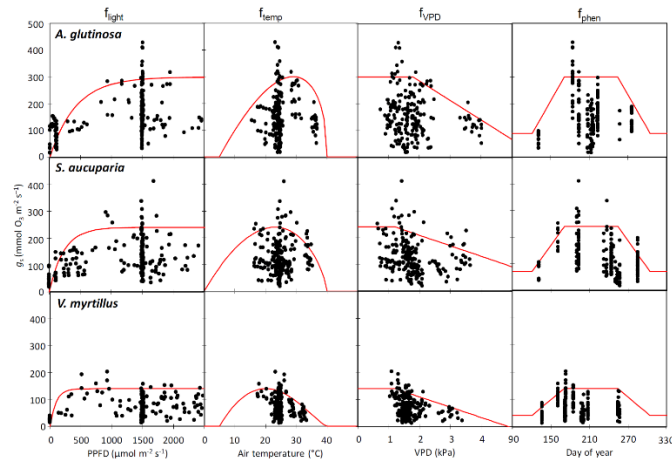

Figure 5. Parameterization of f_{light}, f_{temp}, f_{VPD}, and f_{phen} in stomatal conductance model for *Alnus glutinosa*, *Sorbus aucuparia,* and *Vaccinium myrtillus* exposed to three levels of O_3 concentration (AA, ambient O_3 concentration 1.5 × AA, and 2.0 × AA). Red lines show model functions and black points show measured stomatal conductance.

3.4. Dose-Response Relationship for Plant Injury Index

In *A. glutinosa*, the first criterion (Y-intercept = 0 included in C.I.) was reached in the regressions between PII and AOT40 or POD_{0-7}. Among these indices, POD_7 had the highest R^2 (0.54) (Table S1). On the one hand, the CL corresponding to PII = 5 based on POD_7 was 8.1 mmol m^{-2} (Figure 6) and, on the other hand, the AOT40-based CL was 33 ppm·h. In *S. aucuparia*, the first criterion was achieved for AOT40 and $POD_{0-5.5}$. The highest R^2 value was found in POD_0 (0.87). The CLs in this species were found to be 22 mmol m^{-2} POD_0 and 30 ppm·h AOT40. In *V. myrtillus*, the first criterion was

achieved for AOT40 and POD_{1-4}. POD_1 had the highest R^2 value (0.82), while the exposure-based index AOT40 performed equally well ($R^2 = 0.81$). The CLs was 5.8 mmol m^{-2} POD$_1$ and 20 ppm·h AOT40 in this species.
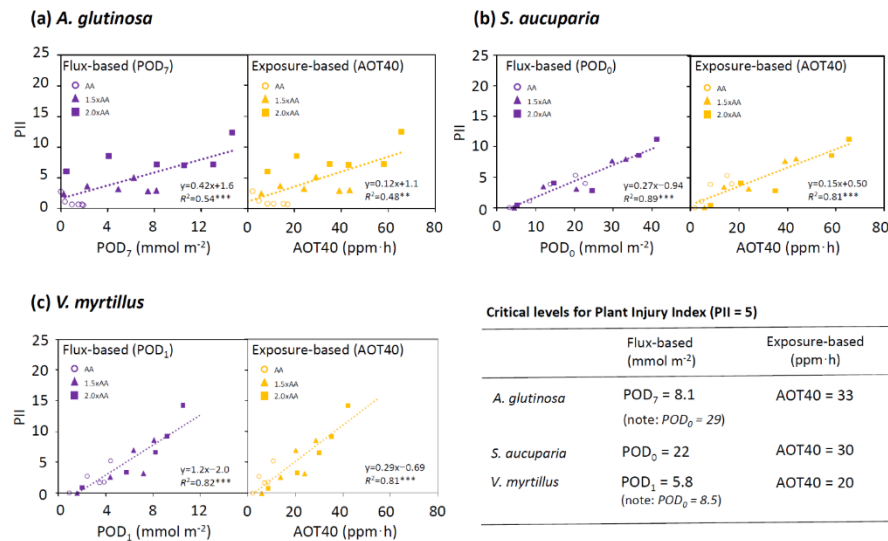

Figure 6. Dose-response relationships for plant injury index (PII) in *Alnus glutinosa*, *Sorbus aucuparia*, and *Vaccinium myrtillus* using two O$_3$ indices, POD$_Y$ (phytotoxic ozone dose above a flux threshold of Y nmol m^{-2} s^{-1}) and AOT40 (accumulated exposure over a threshold of 40 ppb). The critical levels (CLs) corresponding to PII = 5 were also shown. Simple linear regressions were applied. *** $p < 0.001$ and ** $p < 0.01$.

4. Discussion

4.1. New DO3SE Parameterization in Three Deciduous Tree Species

An accurate parameterization of the g_s model is essential to develop a flux-based approach for O$_3$ risk assessment [26,28]. The model performance with new parameterization was comparable to that in previous studies [26,29]. A comparison of the three target species showed that the g_{max} value was relatively high in *A. glutinosa* (300 mmol m^{-2} s^{-1}) as compared with the other species (*S. aucuparia*, 240 mmol m^{-2} s^{-1} and *V. myrtillus*, 140 mmol m^{-2} s^{-1}). This value was within the range for a previous field observation of this species (170 to 380 mmol m^{-2} s^{-1}) [30–32]. A high g_s enhanced stomatal O$_3$ uptake, thus, leading to higher O$_3$ damage [15]. The level of g_{max} in *A. glutinosa* was comparable to that of the other O$_3$-sensitive species such as Oxford poplar clone (340 to 520 mmol m^{-2} s^{-1}) [27,33] and *Fagus crenata* (315 mmol m^{-2} s^{-1}) [34,35].

Interestingly, the parameter *a*, in the f_{light} function, was relatively high in *V. myrtillus* among the three species, suggesting a lower light saturating point of g_s. Karlsson, 1987 [36] and Gerdol et al., 2000 [37] reported a relatively low light saturating point of photosynthesis (200 to 300 µmol m^{-2} s^{-1} of PPFD) in this species. *V. myrtillus* is known as a shade tolerant species [38] while the other two species are light demanding [39,40]. In fact, a high *a* value in f_{light} function was found in other shade tolerant species such as *F. crenata* (*a* = 0.0086) [34], while a lower *a* was obtained in a light-demanding poplar clone (*Populus maximowiczii* Henry x *berolinensis* Dippel, *a* = 0.0020) [27].

In the afternoon, a high VPD often closes stomata together with high air temperature [41]. This was supported by the parameters in f_{VPD} and f_{temp} for the three species. In fact, g_s was decreased by 29%, 29%, and 49%, in *A. glutinosa*, *S. aucuparia*, and *V. myrtillus*, respectively, when VPD reached 3 kPa. In addition, g_s was decreased by 13%, 38%, and 68%, in *A. glutinosa*, *S. aucuparia*, and *V. myrtillus*, respectively, when air temperature reached 35 °C. Since ambient O$_3$ concentrations were elevated in the afternoon, those functions were fundamental for the stomatal O$_3$ flux calculation [28].

4.2. Flux-Based Assessment of Ozone Visible Injury

The foliar symptoms of *A. glutinosa*, *S. aucuparia*, and *V. myrtillus* in this experiment were similar to those observed in the field at ambient O_3 levels [8]. The first foliar symptoms were observed in May in all species exposed to $2.0 \times O_3$. The onset occurred at 5 to 9 ppm·h AOT40. This is supported by the findings in previous studies where 5 to 10 ppm·h AOT40 caused an emergence of O_3 visible injury for sensitive tree species such as *F. sylvatica* [11]. In addition, the present study found that approximately 4 mmol m^{-2} POD$_0$ was enough to cause the onset of O_3 visible injury regardless of tree species. *A. glutinosa* with a high g_{max} quickly reached this critical point of POD$_0$ and showed the first symptom earlier than the other two species. In species with a high g_s, the O_3 dose can easily exceed the metabolic capacity for detoxification, and therefore can quickly cause O_3 visible injury [42].

After the onset, the O_3 visible injury expanded to the plant level in all three species as confirmed by the increase in PII values. The increases of PII were well correlated with flux-based indices (POD$_Y$) in each species. The POD$_Y$ showed a higher R^2 than AOT40, suggesting that POD$_Y$ was better than AOT40 to assess PII. This is supported by the fact that O_3 impacts are more closely related to O_3 uptake than to external O_3 exposure [15]. Previous studies suggested a threshold Y as an assumed threshold below which stomatal O_3 flux by the plant may be detoxified [16]. The result shows that Y was relatively higher in *A. glutinosa* (Y = 7) as compared with other two species (Y = 0 to 1). This suggests that *A. glutinosa* can have a higher capacity for O_3 detoxification than the other two species, although this species had a high stomatal O_3 uptake.

Sicard et al., 2016 [17] indicated that 22 mmol m^{-2} of POD$_0$ corresponded to 5% visible injury in O_3-sensitive deciduous *F. sylvatica* according to field measurements. Our results in *A. glutinosa* and *S. aucuparia* support their findings because the CLs corresponding to PII = 5 on the basis of POD$_0$ were 22 and 29 mmol m^{-2} in *A. glutinosa* and *S. aucuparia*, respectively. However, the CL in *V. myrtillus* was much lower than that of the other two species. On the basis of PII, *V. myrtillus* was more sensitive to O_3 than *A. glutinosa* and *S. aucuparia*. This is because *V. myrtillus* had a dramatic increase in PII from June to July. Although it had a relatively low g_s and thus low stomatal O_3 uptake, this species was highly susceptible to O_3 in these months. *V. myrtillus* had a vegetative stage in May and then flowering and fruiting stages from June to July [43]. In fact, previous studies found that the capacity to detoxify O_3 was lower when the plants were flowering or producing fruits [44–46].

The seasonal dynamics of PII differed among the species. In *S. aucuparia* and *V. myrtillus*, the PII values showed a monotonic increase, while *A. glutinosa* had a rather constant PII during June to August. Novak et al., 2003 [13] reported that several species (*Populus nigra*, *Prunus avium*, and *Salix alba*) similarly had a leveling or even decreasing trend of total injured leaf area during the season. In general, O_3 visible injury usually appears on older leaves [4]. However, new leaf formation in *A. glutinosa* was significantly increased by elevated O_3, while damaged old leaves were shed. This new leaf growth can alleviate the expansion of O_3 visible injury at the plant level in *A. glutinosa*. An accelerated leaf turnover can be considered as a compensation response to O_3 stress in plants with indeterminate growth pattern [20]. However, PII in $2.0 \times$ AA was still significantly higher than that in AA in *A. glutinosa*, suggesting that such leaf growth did not fully compensate for the O_3 damage.

5. Conclusions

The present O_3 FACE experiment successfully confirmed O_3 visible injury in three cool-temperate deciduous tree species, *A. glutinosa*, *S. aucuparia*, and *V. myrtillus*. The onset of O_3 visible injury in these species required 4.0 mmol m^{-2} POD$_0$ and 5.5 to 9.0 ppm·h AOT40. The timing of the first symptom onset among the species was determined by the amount of stomatal O_3 uptake. The early emergence of O_3 visible injury in *A. glutinosa* was related to high g_s; however, PII was affected not only by stomatal O_3 uptake but also by other species-specific ecophysiological traits. The dynamics of PII suggest that an increased fructification (flowering, fruiting) can weaken the state of the *V. myrtillus* tree, then, finally the trees can be more sensitive to O_3 [47]. In addition, PII values in *A. glutinosa* were affected by its indeterminate growth pattern, and a new leaf formation alleviated the expansion of O_3 visible injury at

the plant level in this species. Nevertheless, O_3 impacts on PII were better explained by the flux-based index, POD_Y, than by the exposure-based index, AOT40, especially in *A. glutinosa*, although it changed in a complex manner. The CLs corresponding to PII = 5 were 8.1 mmol m^{-2} POD_7 in *A. glutinosa*, 23 mmol m^{-2} POD_0 in *S. aucuparia*, and 5.8 mmol m^{-2} POD_1 in *V. myrtillus*.

Forest trees also suffer from other climate change factors such as elevated CO_2, nitrogen deposition, warming, the risk of flooding, drought, and forest fire [42]. The interactions between O_3 and other climate change factors are crucial to establish the species-specific O_3 flux-effect relationship for the O_3 risk assessment.

Supplementary Materials: The following are available online at http://www.mdpi.com/1999-4907/11/1/82/s1, Figure S1: Comparison between measured and estimated g_s in *Alnus glutinosa*, *Sorbus aucuparia* and *Vaccinium myrtillus*. Table S1: Summary for R^2 and the information of confidential interval (C.I.) in exposure or flux-based dose-response functions for plant injury index (PII).

Author Contributions: Y.H., P.S., A.D.M., and E.P. conceived the study; Y.H. and E.C. carried out the experiment and collected the data; Y.H., B.M. and S.M. undertook the statistical analyses. All authors were involved in writing the paper, although Y.H. took a lead role. All authors have read and agreed to the published version of the manuscript.

Conflicts of Interest: The authors declare no conflict of interest.

References

1. Grulke, N.E.; Heath, R.L. Ozone effects on plants in natural ecosystems. *Plant Biol.* **2019**. [CrossRef] [PubMed]
2. Lefohn, A.S.; Malley, C.S.; Smith, L.; Wells, B.; Hazucha, M.; Simon, H.; Naik, V.; Mills, G.; Schultz, M.G.; Paoletti, E.; et al. Tropospheric ozone assessment report: Global ozone metrics for climate change, human health, and crop/ecosystem research. *Elem. Sci. Anthr.* **2018**, *6*, 28. [CrossRef] [PubMed]
3. Mills, G.; Pleijel, H.; Malley, C.S.; Sinha, B.; Cooper, O.; Schultz, M.; Neufeld, H.S.; Simpson, D.; Sharps, K.; Feng, Z.; et al. Tropospheric Ozone Assessment Report: Present day tropospheric ozone distribution and trends relevant to vegetation. *Elem. Sci. Anthr.* **2018**, *6*, 47. [CrossRef]
4. Paoletti, E.; Ferrara, A.M.; Calatayud, V.; Cerveró, J.; Giannetti, F.; Sanz, M.J.; Manning, W.J. Deciduous shrubs for ozone bioindication: *Hibiscus syriacus* as an example. *Environ. Pollut.* **2009**, *157*, 865–870. [CrossRef]
5. Hoshika, Y.; Omasa, K.; Paoletti, E. Whole-tree water use efficiency is decreased by ambient ozone and not affected by O_3-induced stomatal sluggishness. *PLoS ONE* **2012**, *7*, e39270. [CrossRef]
6. Innes, J.L.; Skelly, J.M.; Schaub, M. Ozone and broadleaved species. In *A Guide to the Identification of Ozone-Induced Foliar Injury*; Paul Haupt Verlag: Bern, Switzerland, 2001.
7. Feng, Z.; Sun, J.; Wan, W.; Hu, E.; Calatayud, V. Evidence of widespread ozone-induced visible injury on plants in Beijing, China. *Environ. Pollut.* **2014**, *193*, 296–301. [CrossRef]
8. Paoletti, E.; Alivernini, A.; Anav, A.; Badea, O.; Carrari, E.; Chibulescu, S.; Conte, A.; Ciriani, M.L.; Dalstein-Richier, L.; De Marco, A.; et al. Toward stomatal–flux based forest protection against ozone: The MOTTLES approach. *Sci. Tot. Environ.* **2019**, *691*, 516–527. [CrossRef]
9. Fuhrer, J.; Skärby, L.; Ashmore, M.R. Critical levels for ozone effects on vegetation in Europe. *Environ. Pollut.* **1997**, *97*, 91–106. [CrossRef]
10. Hůnová, I.; Schreiberová, M. Ambient ozone phytotoxic potential over the Czech forests as assessed by AOT40. *iForest Biogeosci. For.* **2012**, *5*, 153–162. [CrossRef]
11. Baumgarten, M.; Werner, H.; Häberle, K.-H.; Emberson, L.D.; Fabian, P.; Matyssek, R. Seasonal ozone response of mature beech trees (*Fagus sylvatica*) at high altitude in the Bavarian forest (Germany) in comparison with young beech grown in the field and in phytotrons. *Environ. Pollut.* **2000**, *109*, 431–442. [CrossRef]
12. Van der Heyden, D.; Skelly, J.; Innes, J.; Hug, C.; Zhang, J.; Landolt, W.; Bleuler, P. Ozone exposure thresholds and foliar injury on forest plants in Switzerland. *Environ. Pollut.* **2001**, *111*, 321–331. [CrossRef]

13. Novak, K.; Skelly, J.M.; Schaub, M.; Kräuchi, N.; Hug, C.; Landolt, W.; Bleuler, P. Ozone air pollution and foliar injury development on native plants of Switzerland. *Environ. Pollut.* **2003**, *125*, 41–52. [CrossRef]

14. Calatayud, V.; Cerveró, J.; Sanz, M.J. Foliar, physiological and growth responses of four maple species exposed to ozone. *Wat. Air Soil Pollut.* **2007**, *185*, 239–254. [CrossRef]

15. Paoletti, E. Ozone impacts on forests. In *CAB Reviews: Perspectives in Agriculture, Veterinary Science, Nutrition and Natural Resources*; CABI: Wallingford, UK, 2007.

16. CLRTAP. Mapping Critical Levels for Vegetation, Chapter III of Manual on methodologies and criteria for modelling and mapping critical loads and levels and air pollution effects, risks and trends, 2017. In *UNECE Convention on Long-Range Transboundary Air Pollution*; Programme Coordinating Centre, Federal Research Centre for Forestry and Forest Products: Hamburg, Germany, 2017; Available online: www.icpmapping.org (accessed on 8 November 2019).

17. Sicard, P.; De Marco, A.; Dalstein-Richier, L.; Tagliaferro, F.; Paoletti, E. An epidemiological assessment of stomatal ozone flux-based critical levels for visible ozone injury in Southern European forests. *Sci. Tot. Environ.* **2016**, *541*, 729–741. [CrossRef]

18. Paoletti, E. Impact of ozone on Mediterranean forests: A review. *Environ. Pollut.* **2006**, *144*, 463–474. [CrossRef]

19. Schaub, M.; Calatayud, V. Assessment of visible foliar injury induced by ozone. In *Forest Monitoring: Methods for Terrestrial Investigations in Europe with an Overview of North America and Asia*; Ferretti, M., Fischer, R., Eds.; Elsevier: London, UK, 2013; pp. 205–221.

20. Pell, E.J.; Brendley, B.W.; Sinn, J.P. Ozone-induced accelerated foliar senescence: Implications for toxicity and compensation. In *Proceedings 1995 Meeting of the Northern Global Change Program*; Hom, J., Birdsey, R., O'Brian, K., Eds.; Gen. Tech. Rep. NE-214; U.S. Department of Agriculture, Forest Service, Northeastern Forest Experiment Station: Radnor, PA, USA, 1996; pp. 13–19.

21. Hoshika, Y.; De Carlo, A.; Baraldi, R.; Neri, L.; Carrari, E.; Agathokleous, E.; Zhang, L.; Fares, S.; Paoletti, E. Ozone-induced impairment of night-time stomatal closure in O_3-sensitive poplar clone is affected by nitrogen but not by phosphorus enrichment. *Sci. Tot. Environ.* **2019**, *692*, 713–722. [CrossRef]

22. Vogel, C.S.; Curtis, P.S.; Thomas, R.B. Growth and nitrogen accretion of dinitrogen-fixing *Alnus glutinosa* (L.) Gaertn. under elevated carbon dioxide. *Plant Ecol.* **1997**, *130*, 63–70. [CrossRef]

23. Heide, O.M. Temperature rather than photoperiod controls growth cessation and dormancy in *Sorbus* species. *J. Exp. Bot.* **2011**, *62*, 5397–5404. [CrossRef]

24. Selås, V.; Sønsteby, A.; Heide, O.M.; Opstad, N. Climatic and seasonal control of annual growth rhythm and flower formation in *Vaccinium myrtillus* (Ericaceae), and the impact on annual variation in berry production. *Plant Ecol. Evolut.* **2015**, *148*, 350–360. [CrossRef]

25. Paoletti, E.; Materassi, A.; Fasano, G.; Hoshika, Y.; Carriero, G.; Silaghi, D.; Badea, O. A new-generation 3D ozone FACE (Free Air Controlled Exposure). *Sci. Tot. Environ.* **2017**, *575*, 1407–1414. [CrossRef]

26. Alonso, R.; Elvira, S.; Sanz, M.J.; Gerosa, G.; Emberson, L.D.; Bermejo, B.; Gimeno, B.S. Sensitivity analysis of a parameterization of the stomatal component of the DO_3SE model for *Quercus ilex* to estimate ozone fluxes. *Environ. Pollut.* **2008**, *155*, 473–480. [CrossRef] [PubMed]

27. Hoshika, Y.; Carrari, E.; Zhang, L.; Carriero, G.; Pignatelli, S.; Fasano, G.; Materassi, A.; Paoletti, E. Testing a ratio of photosynthesis to O_3 uptake as an index for assessing O_3-induced foliar visible injury in poplar trees. *Environ. Sci. Pollut. Res.* **2018**, *25*, 8113–8124. [CrossRef] [PubMed]

28. Emberson, L.D.; Büker, P.; Ashmore, M.R. Assessing the risk caused by ground level ozone to European forest trees: A case study in pine, beech and oak across different climate regions. *Environ. Pollut.* **2007**, *147*, 454–466. [CrossRef] [PubMed]

29. Xu, Y.; Shang, B.; Yuan, X.; Feng, Z.; Calatayud, V. Relationships of CO_2 assimilation rates with exposure- and flux-based O_3 metrics in three urban tree species. *Sci. Tot. Environ.* **2018**, *613–614*, 233–239. [CrossRef]

30. Oleksyn, J.; Karolewski, P.; Giertych, M.J.; Zytkowiak, R.; Reich, P.B.; Tjoelker, M.G. Primary and secondary host plants differ in leaf-level photosynthetic response to herbivory: Evidence from *Alnus* and *Betula* grazed by the alder beetle, *Agelastica alni. New Phytol.* **1998**, *140*, 239–249. [CrossRef]

31. Kučerová, A.; Pokorný, J.; Radoux, M.; Nemcova, M.; Cadelli, D.; Dušek, J. Evapotranspiration of small-scale constructed wetlands planted with ligneous species. In *Transformations of Nutrients in Natural and Constructed Wetlands*; Vymazal, J., Ed.; Backhuys Publishers: Kerkwerve, The Netherlands, 2001; pp. 413–427.

32. Kupper, P.; Ivanova, H.; Söber, A.; Rohula-Okunev, G.; Sellin, A. Night and daytime water relations in five fast-growing tree species: Effects of environmental and endogenous variables. *Ecohydrology* **2017**, *11*, e1927. [CrossRef]

33. Marzuoli, R.; Gerosa, G.; Desotgiu, R.; Bussotti, F.; Ballarin-Denti, A. Ozone fluxes and foliar injury development in the ozone-sensitive poplar clone Oxford (*Populus maximowiczii* x *Populus berolinensis*). *Tree Physiol.* **2009**, *29*, 67–76. [CrossRef]

34. Hoshika, Y.; Watanabe, M.; Inada, N.; Koike, T. Modeling of stomatal ozone conductance for estimating ozone uptake of *Fagus crenata* under experimentally enhanced free-air ozone exposure. *Wat. Air Soil Pollut.* **2012**, *223*, 3893–3901. [CrossRef]

35. Hoshika, Y.; Watanabe, M.; Inada, N.; Koike, T. Effects of ozone-induced stomatal closure on ozone uptake and ist changes due to leaf age in sun and shade leaves of Siebold's beech. *J. Agric. Meteorol.* **2015**, *71*, 218–226. [CrossRef]

36. Karlsson, P.S. Niche differentiation with respect to light utilization among coexisting dwarf shrubs in a subarctic woodland. *Polar Biol.* **1987**, *8*, 35–39. [CrossRef]

37. Gerdol, R.; Iacumin, P.; Marchesini, R.; Bragazza, L. Water- and nutrient-use efficiency of a deciduous species, *Vaccinium myrtillus*, and an evergreen species, *V. vitis-idaea*, in a subalpine dwarf shrub heath in the southern Alps, Italy. *Oikos* **2000**, *88*, 19–32. [CrossRef]

38. Tonteri, T.; Salemaa, M.; Rauto, P.; Hallikainen, V.; Korpela, L.; Merilä, P. Forest management regulates temporal change in the cover of boreal plant species. *For. Ecol. Manag.* **2016**, *381*, 115–124. [CrossRef]

39. Claessens, H.; Oosterbaan, A.; Savill, P.; Rondeux, J. A review of the characteristics of black alder (*Alnus glutinosa* (L.) Gaertn.) and their implications for silvicultural practices. *Forestry* **2010**, *83*, 163–175. [CrossRef]

40. Giertych, M.; Karolewski, P.; Oleksyn, J. Carbon allocation in seedlings of deciduous tree species depends on their shade tolerance. *Acta Physiol. Plant.* **2015**, *37*, 216. [CrossRef]

41. Larcher, W. *Physiological Plant Ecology*, 4th ed.; Springer: New York, NY, USA, 2003.

42. Matyssek, R.; Clarke, N.; Cudlin, P.; Mikkelsen, T.N.; Tuovinen, J.P.; Wieser, G.; Paoletti, E. Climate Change, Air Pollution and Global Challenges: Understanding and persPectives from Forest Research. In *Developments in Environmental Science*; Elsevier: Amsterdam, The Netherlands, 2013; 622p.

43. Pellegrini, E.; Hoshika, Y.; Paoletti, E. Ozone effects on the quality of Common Bilberry fruits. Unpublished work.

44. Vandermeiren, K.; De Temmerman, L.; Hookham, N. Ozone sensitivity of *Phaseolus vulgaris* in relation to cultivar differences, growth stage and growing conditions. *Wat. Air Soil Pollut.* **1995**, *85*, 1455–1460. [CrossRef]

45. Morgan, P.B.; Ainsworth, E.A.; Long, S.P. How does elevated ozone impact soybean? A meta-analysis of photosynthesis, growth and yield. *Plant Cell Environ.* **2003**, *26*, 1317–1328. [CrossRef]

46. Feng, Z.; Pang, J.; Nouchi, I.; Kobayashi, K.; Yamakawa, T.; Zhu, J. Apoplastic ascorbate contributes to the differential ozone sensitivity in two varieties of winter wheat under fully open-air field conditions. *Environ. Pollut.* **2010**, *158*, 3539–3545. [CrossRef]

47. Braun, S.; Schindler, C.; Rihm, B. Growth trends of beech and Norway spruce in Switzerland: The role of nitrogen deposition, ozone, mineral nutrition and climate. *Sci. Tot. Environ.* **2017**, *599–600*, 637–646. [CrossRef]